

# Kinetic Studies of Plasma Chemical Fuel Oxidation in Nanosecond Pulsed Discharges by Single and Two Photon Laser Induced Fluorescence

Zhiyao Yin<sup>1</sup>, Aaron Montello<sup>1</sup>, Sherrie Bowman<sup>1</sup>,  
Campbell D. Carter<sup>3</sup>, Igor V. Adamovich<sup>1</sup>, Walter R. Lempert<sup>3</sup>

<sup>1</sup> *Department of Mechanical & Aerospace Engineering, <sup>2</sup> Departments of Mechanical & Aerospace Engineering and Chemistry, The Ohio State University, Columbus, OH U.S.A.*

<sup>3</sup> *U.S. Air Force Research Laboratory, Wright-Patterson AFB, OH U.S.A*

## Abstract

Single and two photon Laser Induced Fluorescence (LIF) spectroscopy is used for measurements of the hydroxyl radical (OH) and atomic oxygen number densities, respectively, in nanosecond pulsed nonequilibrium discharges. In the case of OH LIF rotational temperatures are also obtained, which are found to agree well with temperatures inferred from Coherent Anti-Stokes Raman Spectroscopy (CARS). The temporal evolution of OH and temperature after application of a burst of 50 nsec pulses at 10 kHz repetition rate in fuel lean hydrogen, methane, ethylene, and propane-air plasmas at  $P = 100$  Torr is compared to predictions from a plasma-chemical fuel oxidation code. It is found that the kinetic mechanisms developed by A. Konnov provide the best overall agreement with the experimental data. Atomic oxygen data in 40 Torr hydrogen-air mixtures indicates significant low temperature chemical oxidation.

## 1. Introduction

Nonequilibrium plasmas formed by nanosecond (nsec) duration pulsed discharges provide an excellent platform for fundamental study of the kinetics of plasma-chemical fuel oxidation at low temperature. The peak *reduced* electric field,  $(E/N)$ , in these discharges is of the order of  $10^2$ - $10^3$  Td ( $1 \text{ Td} = 10^{-17} \text{ V} \cdot \text{cm}^2$ ), which enhances electronic excitation and dissociation of gas molecules, resulting in efficient generation of radical species at temperatures much lower than under ordinary equilibrium conditions. Time resolved temperature and intermediate radical species measurements, therefore, provide a stringent quantitative assessment of the detailed predictive capability of plasma-chemical oxidation models at low temperatures, of order 400 – 800 K, a regime where combustion chemistry model validation is typically lacking.

In this talk time and space-resolved data is presented in two nsec pulsed plasma-chemical test cells, both of which are designed to readily accommodate laser-based diagnostic methods as well as to minimize spatial non-uniformities in the plasma. Specifically, measurements are performed in (i), a plane-to-plane discharge under fuel lean conditions in which the fuel-air mixtures are preheated to temperatures as high as  $\sim 500$  K; and (ii), a diffuse pin-to-pin discharge, initially at room temperature. In the plane-to-plane geometry, the temporal evolution of hydroxyl radical (OH),

determined by single photon Laser Induced Fluorescence (LIF) and rotational/translational temperature, determined by LIF and Coherent anti-Stokes Raman Spectroscopy (CARS), in fuel lean  $\text{H}_2$ -air and hydrocarbon-air mixtures is compared to predictions of a plasma-chemical modelling code, which has been presented previously [1-3] but here has been modified to include several different published chemical kinetic mechanisms. It is found that the kinetic mechanisms for  $\text{H}_2$ -air,  $\text{CH}_4$ -air, and  $\text{C}_2\text{H}_4$ -air developed by A. Konnov [4,5] provide the best overall agreement with OH measurements. In  $\text{C}_3\text{H}_8$ -air, none of the hydrocarbon chemistry mechanisms employed were found to agree well with the data. In the pin-to-pin geometry, Two Photon Laser Induced Fluorescence (TALIF) measurements of atomic oxygen are performed.

## 2. OH and Temperature Measurements

The experimental setup used in the present work, shown schematically in Fig. 1, is described in detail in [6]. Briefly, the cell consists of a 280-mm-long, 22 mm x 10 mm rectangular cross section quartz channel with wall thickness of 1.75 mm. Two plane quartz windows are fused to the ends of the channel, providing optical access in the axial direction. A right-angle fused silica prism is placed along the channel to provide optical access from the side. The entire assembly is heated in a tube furnace to improve plasma stability. A quartz coil is used to

Report Documentation Page				Form Approved OMB No. 0704-0188		
Public reporting burden for the collection of information is estimated to average 1 hour per response, including the time for reviewing instructions, searching existing data sources, gathering and maintaining the data needed, and completing and reviewing the collection of information. Send comments regarding this burden estimate or any other aspect of this collection of information, including suggestions for reducing this burden, to Washington Headquarters Services, Directorate for Information Operations and Reports, 1215 Jefferson Davis Highway, Suite 1204, Arlington VA 22202-4302. Respondents should be aware that notwithstanding any other provision of law, no person shall be subject to a penalty for failing to comply with a collection of information if it does not display a currently valid OMB control number.						
1. REPORT DATE <b>JUL 2013</b>		2. REPORT TYPE <b>N/A</b>		3. DATES COVERED <b>-</b>		
4. TITLE AND SUBTITLE <b>Kinetic Studies of Plasma Chemical Fuel Oxidation in Nanosecond Pulsed Discharges by Single and Two Photon Laser Induced Fluorescence</b>				5a. CONTRACT NUMBER		
				5b. GRANT NUMBER		
				5c. PROGRAM ELEMENT NUMBER		
6. AUTHOR(S)				5d. PROJECT NUMBER		
				5e. TASK NUMBER		
				5f. WORK UNIT NUMBER		
7. PERFORMING ORGANIZATION NAME(S) AND ADDRESS(ES) <b>Department of Mechanical &amp; Aerospace Engineering, The Ohio State University, Columbus, OH U.S.A.</b>				8. PERFORMING ORGANIZATION REPORT NUMBER		
9. SPONSORING/MONITORING AGENCY NAME(S) AND ADDRESS(ES)				10. SPONSOR/MONITOR'S ACRONYM(S)		
				11. SPONSOR/MONITOR'S REPORT NUMBER(S)		
12. DISTRIBUTION/AVAILABILITY STATEMENT <b>Approved for public release, distribution unlimited</b>						
13. SUPPLEMENTARY NOTES <b>See also ADA594770. International Conference on Phenomena in Ionized Gases (31st) (ICPIG) Held in Granada, Spain on 14-19 July 2013</b>						
14. ABSTRACT <b>Single and two photon Laser Induced Fluorescence (LIF) spectroscopy is used for measurements of the hydroxyl radical (OH) and atomic oxygen number densities, respectively, in nanosecond pulsed nonequilibrium discharges. In the case of OH LIF rotational temperatures are also obtained, which are found to agree well with temperatures inferred from Coherent Anti-Stokes Raman Spectroscopy (CARS). The temporal evolution of OH and temperature after application of a burst of 50 nsec pulses at 10 kHz repetition rate in fuel lean hydrogen, methane, ethylene, and propane-air plasmas at P = 100 Torr is compared to predictions from a plasma-chemical fuel oxidation code. It is found that the kinetic mechanisms developed by A. Konnov provide the best overall agreement with the experimental data. Atomic oxygen data in 40 Torr hydrogen-air mixtures indicates significant low temperature chemical oxidation.</b>						
15. SUBJECT TERMS						
16. SECURITY CLASSIFICATION OF:				17. LIMITATION OF ABSTRACT <b>SAR</b>	18. NUMBER OF PAGES <b>4</b>	19a. NAME OF RESPONSIBLE PERSON
a. REPORT <b>unclassified</b>	b. ABSTRACT <b>unclassified</b>	c. THIS PAGE <b>unclassified</b>				

preheat the fuel-air mixture to the furnace temperature. Two 14 mm x 60 mm rectangular plate copper electrodes, rounded at the edges, are placed on the top and bottom of the quartz channel, which are powered with an FID GmbH FPG 60-100MC4 pulse generator. In this work, the pulser is operated in repetitive burst mode, producing bursts of 50 ~30 kV – 5 nsec duration pulses at a pulse repetition rate of 10 kHz and burst repetition rate of 5 Hz.

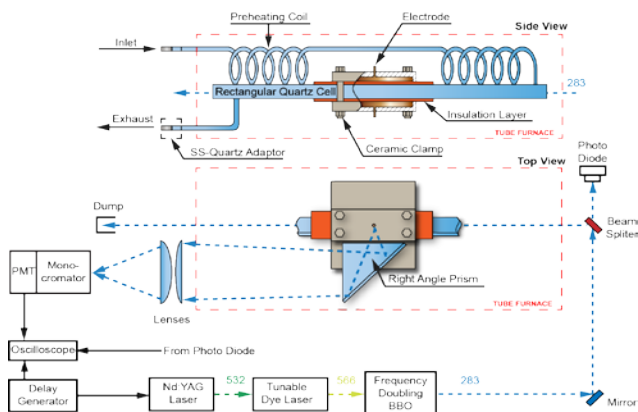


Figure 1: Schematic diagram of plane-to-plane test cell and OH LIF apparatus.

Details of the OH LIF diagnostic are given in [7]. Briefly, OH LIF excitation spectra are obtained by slowly scanning the output of a frequency doubled tunable dye laser in the vicinity of 283 nm, corresponding to excitation of ro-vibronic transitions within the  $X^2\Pi - A^2\Sigma^+$  (1,0) system of OH. Fluorescence emission from the (0,0) and (1,1) vibrational bands, in the vicinity of 310 nm, is captured with a standard photomultiplier tube and optical filter. For OH LIF thermometry, the laser is tuned over five primary transitions, as shown in Fig. 2. For a sub-set of the data presented here, temperatures were also obtained using Coherent Anti-Stokes Raman Spectroscopy (CARS), which gave very similar results.

OH concentration is obtained from the  $Q_1(3)$  transition, the integrated intensity from which is converted to absolute OH number density using the measured temperature in combination with a Rayleigh scattering calibration method described in [7].

OH LIF data has been obtained in fuel lean mixtures of  $H_2/air$ ,  $CH_4/air$ ,  $C_2H_4/air$  and  $C_3H_8/air$  over a range of equivalence ratios. In all cases the data is presented as a function of time after the final pulse in a burst of 50 nsec discharge pulses at  $\nu=10$  kHz. The initial temperature and pressure of the preheated mixtures is 500 K and 100 Torr, respectively.

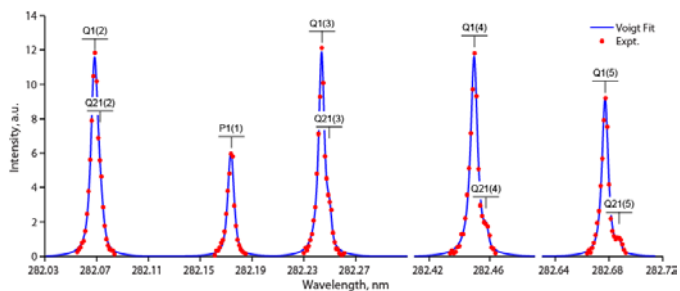


Figure 2: Typical OH LIF excitation spectrum used for temperature measurements. ( $\nu=10$  kHz, 50 pulses).  $H_2$ -air,  $T_0=500$  K,  $P=100$  Torr,  $\phi=0.12$ .

Figure 3 a/b shows  $H_2/air$  data along with modeling predictions using the  $H_2/air$  kinetic mechanisms of Popov [8] and Konnov [4], respectively. Note that the y axis on the left gives the experimental OH number density data whereas the axis on the right shows the modeling predictions. It can be seen that both mechanisms predict the relative data quite well but the Konnov mechanism better predicts the absolute magnitudes. Both mechanisms predict the temperature well.

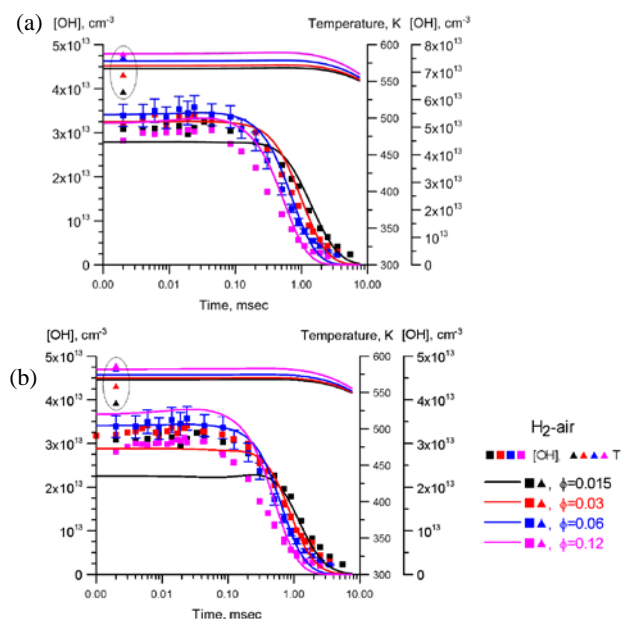


Figure 3: Experimental (left y-axis) and predicted (right y-axis) time-resolved, absolute OH number densities after a  $\nu=10$  kHz, 50-pulse discharge burst in  $H_2$ -air mixtures at  $T_0=500$  K,  $P=100$  Torr, and different equivalence ratios, compared to (a) Popov and (b) Konnov kinetic mechanisms.

Figure 4a/b/c is similar to Fig. 3, but in this case  $CH_4$ -air data is compared to modeling predictions using the GRI Mech 3.0 [9], USC [10], and Konnov mechanisms [5], respectively. Again, while all of the predictions for relative OH temporal evolution are in good accord with measured [OH],

the Konnov mechanism gives the best overall absolute agreement.

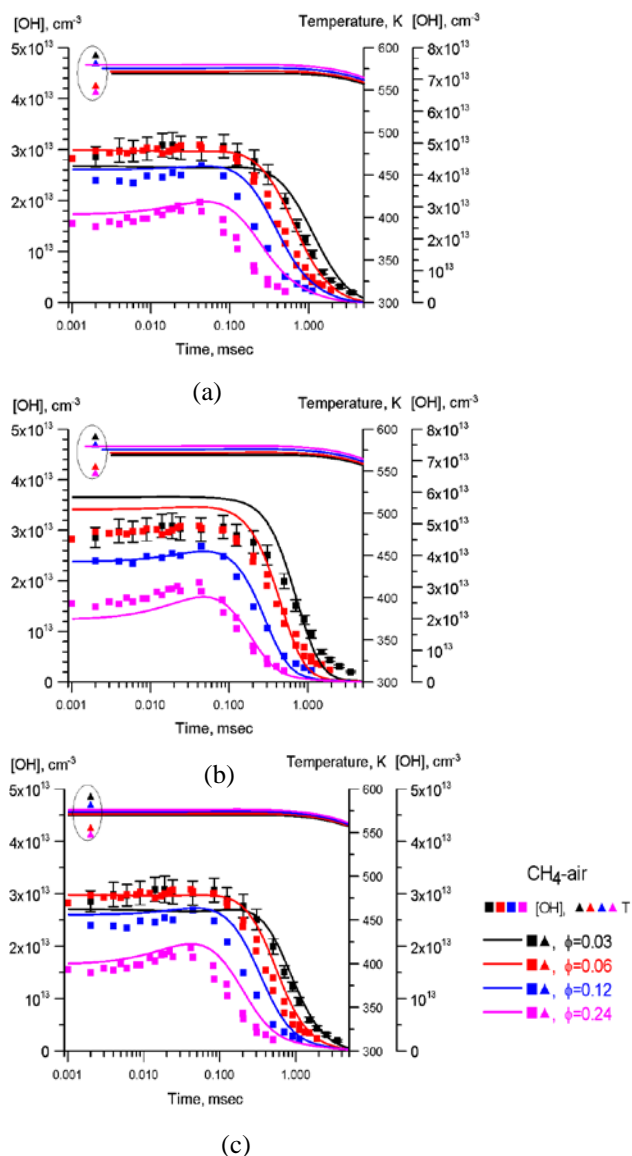


Figure 4: Similar comparison as Fig. 3 but for CH<sub>4</sub>-air using (a) GRI 3.0, (b) USC, and (c) Konnov mechanisms.

Results in C<sub>2</sub>H<sub>4</sub>-air were similar to those in CH<sub>4</sub>-air, although the agreement was somewhat poorer for all kinetic mechanisms. For C<sub>3</sub>H<sub>8</sub>-air mixtures, the relative temporal evolution was not well predicted by any of the kinetic mechanisms and the absolute OH was over-predicted by a factor of ~3, 10, and 6, respectively for the GRI Mech 3.0, USC, and Konnov mechanisms.

### 3. Atomic Oxygen Measurements

Atomic oxygen (O) production and decay is studied in the diffuse single filament pin-to-pin discharge shown in Fig. 5. The discharge produces a stable, reproducible, filament with approximate

dimensions 2-3 mm (diameter) x 10 mm (height), which is sufficiently small to achieve high specific energy loading (~100's of meV/molecule) yet large enough to readily enable optical diagnostic studies and to reduce mass diffusion effects. The spherical electrodes are bare copper, with diameter of ~7.5 mm. The power supply produces ~20 kV peak voltage pulses of ~100 nsec duration and repetition rate  $\nu=50$  Hz. The voltage drops rapidly, however, after discharge breakdown resulting in an effective pulse duration of ~10-20 nsec, based on current flow, and ~8 kV peak voltage. Measurements are performed midway between the electrodes, along the centreline radially.

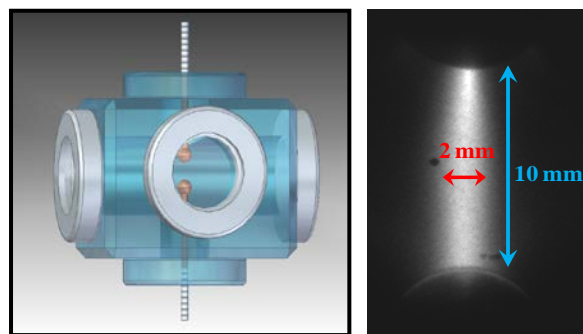


Figure 5: Three dimensional rendering (left) of diffuse single filament discharge cell and representative spontaneous emission image (right). 100 Torr - N<sub>2</sub>.

Absolute O concentrations are measured by Two Photon Absorption Laser Induced Fluorescence (TALIF), which has been described in detail previously [1]. Briefly, O is excited by two photon absorption from the 2p <sup>3</sup>P ground state to the 3p <sup>3</sup>P excited state, with subsequent fluorescence to the 3s <sup>3</sup>S state. Similar to OH LIF, excitation spectra are obtained by slow scanning of the excitation laser in the vicinity of 225.7 nm, which is created by mixing the output of an Nd:YAG pumped dye tunable dye laser with the 355 nm (third harmonic) output of the same Nd:YAG laser. Excitation spectra are then numerically integrated and the relative intensities put on an absolute scale using a xenon calibration technique developed by Niemi et al [11].

Figure 6 shows some initial results for air and H<sub>2</sub> - air mixtures at equivalence ratios in the range  $\phi = 0.07 - 0.43$ . The initial temperature and pressure are 300 K and 40 Torr, respectively, and the coupled pulse energy, based on current-voltage characteristics, is ~0.5 eV/molecule. In all cases the data show absolute O number density as a function of time after initiation of a single nsec discharge pulse. In this initial work, the O data has not yet been corrected for changes in temperature that occur on the time scale of the measurement. Previous

CARS thermometry measurements in a similar pin-to-pin discharge in air, although with a different nsec pulser, resulted in an increase in rotational/translational temperature of  $\sim 200$  K [12]. Increasing temperature affects the inferred [O] through the ideal gas relationship and due to the decrease in the Boltzmann fraction of the ground level of the absorbing transition, which in this case is the lowest level of a triplet. Both effects would tend to increase the inferred [O] values shown in Fig. 6.

While modelling calculations have not yet been performed, some trends are clearly observable in the experimental data. First, the inferred [O] for the shortest time delay measured after discharge initiation,  $\sim 20$   $\mu$ sec, is found to decrease with increasing  $H_2$  mole fraction. Second, the decay O is found to increase rapidly with increasing equivalence ratio, indicating significant chemical reaction. Finally, it appears that the [O] increases slowly at relatively long time scales ( $\sim 0.1$  - 1 msec) after discharge initiation. Modelling predictions are currently in progress which will provide more

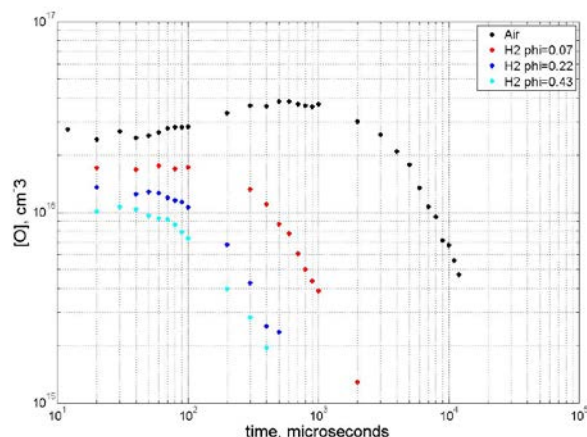


Figure 6: Temporal evolution of O number density in diffuse filament discharge in air and  $H_2$ -air mixtures.  $P = 40$  Torr,  $T_0 = 300$  K.

#### 4. Acknowledgements

The authors acknowledge support of the U.S. Air Force Office of Scientific Research MURI “Fundamental Aspects of Plasma Assisted Combustion” (Chiping Li, technical monitor), by the DOE Low Temperature Plasma Physics Plasma Science Center (Department of Energy, Office of Fusion Energy Science Contract DE-SC0001939, Nirmol Podder, technical monitor), and by the National Science Foundation – DOE Partnership in Basic Plasma Science and Engineering (Steven Gitomer, technical monitor).

#### 5. References

- [1] M. Uddi, N. Jiang, E. Mintusov, I.V. Adamovich, and W.R. Lempert, *Proc. Comb. Inst.* 32 (2009) 929.
- [2] I. Choi, Z. Yin, I.V. Adamovich, and W.R. Lempert, *IEEE Trans. Plas. Sci.* 39 (2011).
- [3] I.A. Kossyi, A. Yu. Kostinsky, A. A. Matveyev, and V.P. Silakov, *Plasma Sources Sci. and Tech.* 1 (1992) 207.
- [4] A. Konnov, *Comb. and Flame* 152 (2008) 507.
- [5] A. Konnov, “Detailed reaction mechanism for small hydrocarbons combustion,” Release 0.5. <http://homepages.vub.ac.be/~akonnov/> (2000).
- [6] Z. Yin, I.V. Adamovich, and W.R. Lempert, *Proc. Comb. Inst.* 34 (2013) 3249.
- [7] Z. Yin, C. Carter, I.V. Adamovich, and W.R. Lempert, AIAA-2013-0432, 51<sup>st</sup> AIAA Aerospace Sciences Meeting, 7-10 January 2013, Grapevine, TX.
- [8] N.A. Popov, *Plasma Physics Reports* 34 (2008) 376.
- [9] [http://www.me.berkeley.edu/gri\\_mech/version30/text30.html](http://www.me.berkeley.edu/gri_mech/version30/text30.html), GRI-Mech 3.0.
- [10] H. Wang, X. You, A.V. Joshi, S.G. Davis, A. Laskin, F. Egolfopoulos, and C.K. Law, USC Mech Version II. [http://ignis.usc.edu/USC\\_Mech\\_II.htm](http://ignis.usc.edu/USC_Mech_II.htm), (2007).
- [11] Niemi, K., V.S. Gathen, and H.F. Dobe. *Plasma Sources Sci. and Tech.* 14 (2005) 386.
- [12] A. Montello, Z. Yin, D. Burnette, I.V. Adamovich, and W.R. Lempert, manuscript in preparation for submission to *J. Phys D*.